

## On the Solute Clustering Effect of Cu to Stimulate Enhanced Age-Hardening in 7000 Series Al-Zn-Mg-Cu

P.V. Liddicoat<sup>1</sup>, S.K. Maloney<sup>2</sup> and S.P. Ringer<sup>1</sup>

<sup>1</sup> Australian Centre for Microscopy & Microanalysis, The University of Sydney, NSW, 2006, Australia.

<sup>2</sup> New Zealand Aluminium Smelters Limited, Invercargill, 2810, New Zealand

Experimentally describing the very first elements of phase transformations, i.e. atomic clustering, is a challenging investigation somewhat constrained by instrument limitations. Recent advancements in atom probe tomography (APT), including specialised algorithms for precise cluster quantification, have revealed complex states of clustering, or solid solution nanostructures, in age-hardened Al alloys that begin in the as-quenched state. Describing how clustering evolves from the as-quenched condition, and to what precipitates specific clustering processes lead to, permits a greater understanding of how to optimise thermo-mechanical treatments and alloy composition to achieve desired properties for designated applications. Specifically, the current study into 7000 series alloys offers an evolutionary insight into the effect of Cu to stimulate increased solute cluster number densities and accelerated solute utilisation. In an alloy of composition Al-2.0Zn-1.9Mg-0.7Cu (at.%) it has been found that precipitation observed in TEM is highly unlikely the sole cause for mechanical property change. During age-hardening substantial hardening reactions may occur when mild, or no, precipitation exists. By accounting for the full structural activity of solute atoms, i.e. whether they are in precipitates, nano-sized clusters (nanoclusters), or the matrix, we have gained an insight into structure to property relationships and have assessed the efficiency of solute utilisation in different structural arrangements.

**Keywords:** 7000 series, age-hardening, atom probe microscopy

### 1. Introduction

In recent work, investigations have been made into the atomic decomposition of the ternary, Al-Zn-Mg, 7000 series Al alloy by a combination of atom probe tomography (APT), transmission electron microscopy (TEM) and positron annihilation lifetime spectroscopy (PALS) [1-4]. When aged at 150 °C, which is above the GP zone solvus temperature determined by Polmear et al. [5], it has been demonstrated that the formation and subsequent evolution of solute-vacancy and solute-solute clusters is linked to the nucleation of meta-stable  $\eta'$  and equilibrium  $\eta$  precipitates. The  $\eta'$  phase has been found to possess varying ratios of Zn:Mg from 1 to 2 and assumed to occupy the structure proposed by Auld and Cousland ( $P\bar{6}m2$ ,  $a=0.496$  nm and  $c=1.402$  nm) whereas the equilibrium phase  $\eta$  is widely considered to possess stoichiometry  $MgZn_2$  and a hexagonal structure;  $P6_3/mmc$ ,  $a=0.520-0.523$  nm and  $c=0.857-0.862$  nm [6-12]. The addition of Cu to 7000 series Al alloys increases strength and, most importantly, improves resistance to stress-corrosion cracking. As a result, the Cu-bearing 7000 series alloys have established wide-spread technological significance [13-14]. Despite the fact that these alloys have been used successfully for over 50 years, much remains uncertain on how Cu modifies the microstructure and so achieves the improved mechanical properties. A feature of certain Cu-bearing Al-Zn-Mg alloys is the onset of a very rapid hardening reaction within the first minute of ageing at select elevated temperatures [13, 15-16]. This initial rapid hardening is usually followed by an incubation period, where the hardness changes little, before increasing again to achieve peak hardening. This two-stage age-hardening curve is in contrast to the single-stage age-hardening that occurs in the ternary alloy. A topical question is: does small additions of Cu introduce new precipitate phases or simply modify the existing microstructure within the ternary Al-Zn-Mg system? Recent studies have demonstrated a combination of both. Precipitate phases usually observed in Al-Cu-Mg alloys have been reported in this quaternary system [16]; GPB

zones which are fully coherent rod-shaped precipitates rich in Cu and Mg, but whose detailed structure and chemistry despite much study still remains [17-21], and the S phase (Cmcm;  $a=0.400$  nm,  $b=0.923$  nm,  $c=0.714$  nm) [22]. Below the GP solvus, Cu has also been observed to introduce ellipsoidal/elongated GP zones in addition to the spherical zones usually observed in Al-Zn-Mg [1, 3]. These observations are significant given that the rapid hardening phenomenon is common to both 7000 and 2000 series [13, 16, 23-25]. At 150 °C (above GP solvus temperature [26]) precipitation onset may be reduced from ~120 to 1 min and result in a near doubling of alloy hardness [13, 16, 25]. Assessments of the hardening contribution from precipitates observable at 1 min, which are native to the Al-Zn-Mg system, are insufficient to explain the hardness increase [13, 16, 25]. It has been proposed that solute cluster hardening may provide for the unaccounted property improvements during this early rapid hardening (ERH) reaction [16, 24-25]. A parameter in the propensity for solute clustering may be related to the concentration of vacancies trapped during the quench. Additions of Cu have been recently demonstrated to stimulate potent super-saturation of vacancies in Al-Zn-Mg-Cu alloys [2]. Featuring environments rich in solute, vacancy-assisted solute diffusion may assist the accelerated kinetics. Vacancies, as well as Cu atoms, have also been proposed to lower the energy barrier for nucleation through misfit strain relief [4, 27-29]. In this investigation the role of Cu in stimulating solute-(solute, vacancy) clustering, precipitate nucleation and early rapid hardening will be explored. Central to this study, in order to achieve sensitive measurements of solute interactions, atom probe microscopy has been used with precise crystallographic reconstruction parameters and atomic cluster specific search algorithms [4, 30-31].

## 2. Experimental methods

Scientific alloys were prepared using conventional ingot metallurgy practice. Alloy compositions were Al-2.0Zn-1.9Mg-0.7Cu and Al-1.9Zn-1.7Mg (at.%). Samples were solution heat treated in a salt bath at 460 °C for 1 h, and quenched immediately into room temperature water. Specimens were transferred and stored in liquid nitrogen. T6 ageing was performed at 150°C for various times in silicone oil. The age hardening response was investigated using a LECO Macro Vickers Hardness Tester LV700 AT under a 5 kg load with a 10 sec dwell period (ASTM E92-82). Specimens for TEM and APT were prepared using standard electropolishing techniques [32-33]. TEM was performed on a Philips CM20 and APT undertaken using an Imago LEAP™ 3000XSi. APT acquisitions were performed at a temperature of 20 K, pulse frequency of 200 kHz, 25% pulse fraction and a 1% evaporation rate. Each individual APT reconstruction was carefully calibrated to crystallographic parameters using lattice spacing for  $k_f$  instead of ring counting [4, 31]. Prior to analysis, low density erosion of zone and pole lines in the APT data was performed [30]; a 100 nearest neighbour (NN) analysis and 22.5 atoms per nm<sup>3</sup> threshold was used. Following careful consideration of the APT clustering algorithms and parameters available, a 1 NN, 2.5 point density, and 0.3 nm d-link core-linkage analysis was used to assess atomic clustering [30]. These parameters were chosen to investigate the direct 1<sup>st</sup> nearest neighbour solute interactions. Atoms within the Al lattice have a largest spacing of ~2.8 nm and on average much lower; it was observed that choosing a higher point density or larger d-link than above reduces the ability to assess direct solute-to-solute chemical interactions. Acquisitions of each ageing condition was repeated a minimum of three times on to ensure consistent activity assessments. Each data set possessed no less than  $\sim 2.0 \times 10^7$  atoms in order to permit a rigorous statistical evaluation of solute interactions. In datasets of this size a stochastic occurrence of clusters will naturally occur. Therefore, to achieve a more sensitive insight into clustering processes, the mean number density of 15 identical, but chemically homogenous, datasets was subtracted from the experimentally observed occurrences. These homogenised datasets were produced by randomly re-assigning each atom's element type, according to nominal composition, and generating a spatially identical but chemically homogenous dataset. This approach has been used successfully in previous APT studies and creates a unique and precise comparison for each acquisition; it also serves to normalise any aberrations that may have been introduced during

acquisition [4, 25, 30, 34]. A 90% confidence interval number density assessment was made by subtracting the average number density from the experimental occurrences, as per above, with the additional subtraction of 1.645 multiplied by the standard deviation. In order to calculate precipitate number density in TEM, convergent beam electron diffraction (CBED) was used to calculate foil volumes and bright field (BF) montages were recorded close to the  $\langle 110 \rangle_\alpha$  zone axis in a

region of uniform brightness and good precipitate contrast [35].

### 3. Age-hardening response

The effect of Cu on the T6 age-hardening response is presented in Fig. 1. The ternary response has been reproduced from reference [4]. In the Cu bearing alloy attention should be drawn to the overall hardness increase and, in particular, the introduction of a dramatic early rapid hardening (ERH) reaction - a  $\sim 88\%$  hardness increase from the as-quenched (AQ) condition in the first minute of ageing.

### 4. Microstructure evolution

The microstructure during ageing at  $150^\circ\text{C}$  has been examined using bright field (BF) and selected area diffraction (SAED) TEM. Two ageing times, As-Quenched (AQ) and 1 min, are presented in Fig. 2. Precipitates with plate and block shaped morphologies that appeared to exhibit  $\{111\}_\alpha$  faceting were observed at 1 min. This onset of precipitation is remarkably different to the non-Cu containing ternary alloy which takes up to 120 min before precipitates are observed in BF TEM [4, 13, 16]. The SAED at 1 min were too weak to confirm precipitate identities. At 120 min diffraction spots in SAED at  $1/3$  and  $2/3$   $\mathbf{g}_{\{220\}_\alpha}$  and sharp streaks through  $\{111\}_\alpha$  indicate the presence of  $\eta'$ . Additional spots along  $\mathbf{g}_{\{220\}_\alpha}$  and  $\mathbf{g}_{\{111\}_\alpha}$  were attributed to  $\eta_1$  and  $\eta_2$ . These observations are consistent with previous reports [13, 16, 25]. The evolution of microstructure has also been observed through the use of APT. While the raw atom

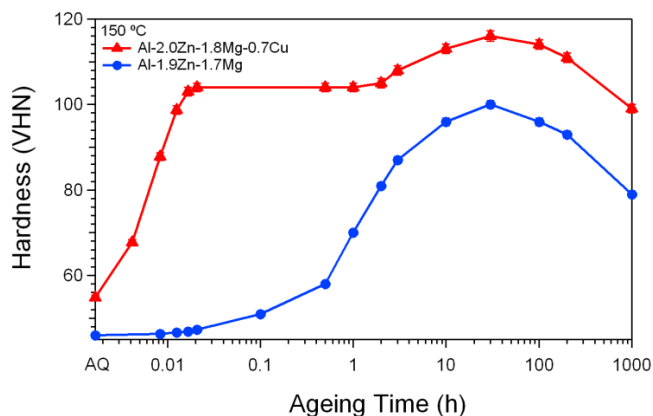


Figure 1 - Age hardening response of alloys at  $150^\circ\text{C}$

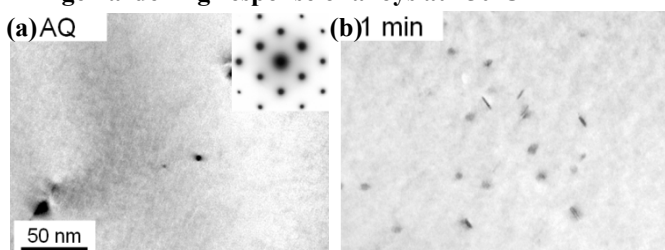


Figure 2 - TEM of Cu bearing alloy at (a) AQ and (b) 1 min

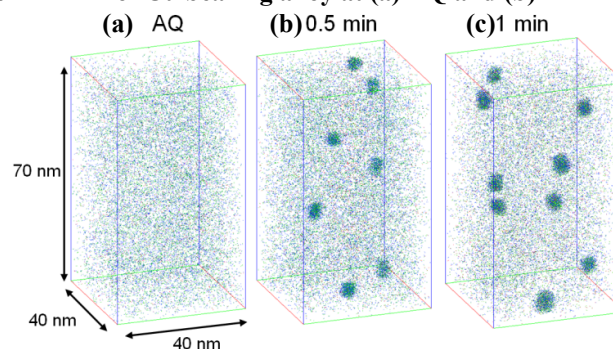


Figure 3 - APT of Cu bearing alloy at (a) AQ (b) 0.5 and (b) 1 min

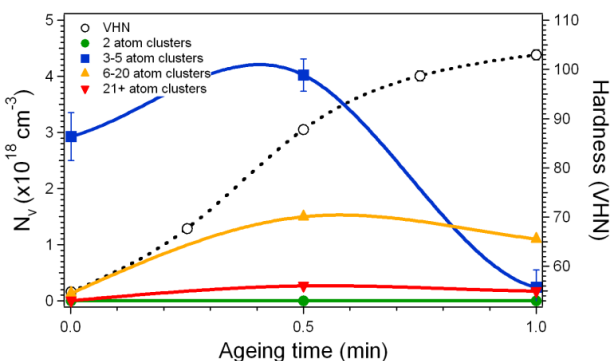


Figure 4 - Number density of cluster groups during 1 min ageing

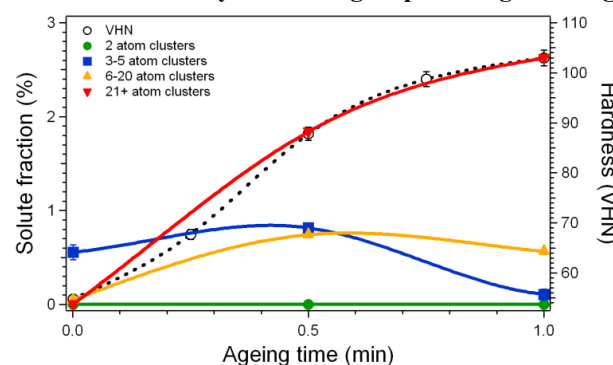


Figure 5 - Solute fraction in cluster groups during 1 min ageing

maps from APT are instructive for initial inspection, the data has been analysed using the core-linkage cluster algorithm to aid in the identification of structure and provide quantitative information [30]. The expected stochastic occurrence of clusters was subtracted from experimental results (see methods). Observed solute clusters were classified into groups based upon the number of atoms and by observing size-based trends in number density during ageing; nanoclusters, medium, small, and dimer correspond to 21+, 6-20, 3-5, and 2 atom clusters, respectively. Solute identified as clustered in the AQ, 0.5 and 1 min condition is presented as cluster maps in Fig. 3, and in terms of number density and solute fraction (fraction of the total solute in the alloy present in 'x' type clusters) in Figs. 4 and 5, respectively. A prominent observation is that the AQ condition features significant number densities of dimer clusters and that there is a 1-to-1 relationship between the evolution of the nanocluster solute fraction and the ERH reaction demonstrated by the alloy. Finding such an 'AQ nanostructure' is consistent with our previous findings in this alloy system [2, 4, 25]. The nanoclusters observed in the 1 min APT cluster map are precipitate-like in dimension to the  $\eta'/\eta$  particles observed in the TEM. To compare the distribution careful quantitative stereology measurements were made of TEM and APT data of the 1 min condition -  $2.53 \pm 0.37 \times 10^{16} \text{ cm}^{-3}$  precipitates in TEM, and  $5.43 \pm 0.25 \times 10^{16} \text{ cm}^{-3}$  nanoclusters in APT (see methods). Over twice the number density of particles were observed in the APT data. This is consistent with our previous analysis of Al-Zn-Mg alloys, where the number density of precipitate-like nanoclusters observed with APT is greater than that detected using conventional TEM [4]. This brings into question the structure and chemistry of the observed precipitate-like particles and their ability to produce contrast in TEM. The structure for all particles was difficult to establish in APT, high-resolution studies revealed plate-shape particles with an elongated axis at  $\sim 54^\circ$  to the  $\{002\}_\alpha$  plane indicative of a  $\{111\}_\alpha$  alignment. This morphology and habit plane is consistent with the meta-stable  $\eta'$  precipitate. Further examination of matrix-particle interface indicates a very high lattice coherency with the matrix; this is not consistent with expectations for the hexagonal structure of the  $\eta'$  phase. These observations do, however, suggest the absence of particle detection in TEM may be due to the chemically diffuse and coherent nature of such nanoscale atomic clusters. Whether these nanoscale clusters of solute are truly 'precipitate', 'zone' or 'solute atom cluster' structures remains an area for future work. As such, they will be referred to as nanoclusters for the remainder of this investigation. Regarding the role of Cu, between 0.5 and 1 min, the Cu content in nanoclusters increases from  $\sim 4.8$  to 8.3%. This indicates that Cu is being preferentially transported into nanoclusters.

## 5. Discussion

Between 0.5 and 1 min ageing the amount of total solute in structures is approximately the same, Fig 5. This is not the case for the microstructure that composes it, however, it substantially alters – a marked reduction in the small and medium cluster solute fractions is near perfectly balanced by the increase of nanoclusters. Combining this information with number density, we observe the numbers of nanoclusters stays near constant leading to the conclusion that the increased solute fraction is a result of nanoclusters growing in size. We find two scenarios most likely to explain the trends observed – (a) the small and medium clusters are the product of an unsustainable clustering force and these unstable embryos, if unable to reach critical nucleation size, dissolve back into the matrix and nanoclusters simply draw more solute from the matrix in order to grow [36]; and/or (b) the small and medium clusters diffuse and integrate with the nanoclusters. Continuing this line of inquiry brings into question the driving forces resulting in the dramatic growth and hardening during this time period. We recently examined the role of vacancies in influencing early Al-Zn-Mg decomposition dynamics and expect a similar role will be played in the present alloy [2, 4]. We were able to provide the quantitative insights and explore the proposition that vacancies inject potent diffusive forces that result in solute clustering and precipitate nucleation [10, 27-29]. The presently investigated quaternary alloy has demonstrated markedly increased hardening and clustering kinetics, for example,  $\sim 3.4\%$  total clustered solute fraction at 0.5 min versus  $\sim 0.8\%$  at the same time in the ternary

alloy. We will now explore to what extent vacancies are influencing these elevated reactions. In the AQ condition, the 0.7Cu at.% addition has been reported to result in over 3 times the number density of vacancies trapped during the quench;  $6.5 \times 10^{17} \text{ cm}^{-3}$  in the ternary,  $21 \times 10^{17} \text{ cm}^{-3}$  in the quaternary [2]. It was further found that the average environment of these vacancies was considerably enriched with solute. The Cu was directly attributed to influencing the retained vacancy concentration and solute-vacancy complexes. The mechanism by which Cu achieves the greater concentration has not been fully resolved. Potential explanations are that Cu may elicit a strong atom to vacancy binding energy in an Al matrix, or it may enhance the trapping potential when acting as part of a solute cluster. The former scenario is favoured for the following reasons: Cu atom-vacancy binding would provide elevated mobility that in turn permits increased solute atom contact and results in the dramatic solute clusters/complexes observed [10, 28-29]; in the latter scenario an unknown force would have to provide rapid clustering before trapping could occur. Contrasting the vacancy activity in the ternary and quaternary alloys, the addition of Cu stimulates a 38% increase in the total solute involved in solute-vacancy complexes [2]. In the quaternary alloy, complexes contain 63% of the total clustered solute in the AQ condition and reduce to 4% by 1 min. During this time solute clustering increases and solute-vacancy complexes decrease as vacancies rapidly extinguish; the thermal excitation of the elevated ageing temperature generates rapid migration of quenched-in vacancies, stimulating clustering, and extinguish at vacancy sinks or within nucleation reactions. The efficiency of the solute utilised to affect a hardness increase has been investigated. Between 0.5 to 1 min the total solute in structures is practically identical - only how the solute is structured changes. At 0.5 min, the solute fraction is half nanoclusters and half small and medium clusters. At 1 min nanoclusters constitute the majority of the solute fraction with the medium clusters making up the remainder. In light of both conditions utilising the same amount of solute, and the absence of any other attributable structures in the alloy, we expect that the nanoclusters are more efficient than the distribution of the medium or small clusters in affecting a hardness increase. Furthermore, considering the 1-to-1 relationship of nanoclusters to hardening response, it is likely that the ERH reaction during this period may in fact solely depend upon the nature of nanoclusters present.

## 6. Conclusion

We set out to investigate how the addition of 0.7 at.% Cu accelerates the kinetics and age-hardening response in this Al-Zn-Mg-Cu alloy. We may now draw the following conclusions:

- An as-quenched nanostructure exists in the alloy. This nanostructure is composed of solute clusters and solute-vacancy complexes which are highly concentrated as a result of Cu addition.
- The potent vacancy concentration is expected to induce vigorous solute clustering and acceleration of nucleation – we propose this is expedited through vacancy-assisted mobility vastly elevating diffusion and by reducing nucleation energy through misfit strain relief.
- The early rapid hardening reaction (~88% increase in 1 min) correlates to the fraction of solute involved in nanoclusters. In the absence other correlative structures, it is suggested that the nature of this nanocluster distribution gives rise to the hardening. It is uncertain whether these nanoclusters are one or more of the following: precipitates, zones or nanometre scale solute atom clusters. Approx. half of the nanoclusters were not visible in conventional BF TEM which may account for previous inaccuracies in calculations of precipitate-hardening contributions.

## Acknowledgements + References

This research was supported by the Australian Research Council. The authors are grateful for the scientific and technical support from the Australian Centre for Microscopy & Microanalysis (ACMM) at The University of Sydney.

- [1] Sha, G. and A. Cerezo, *Early-stage precipitation in Al-Zn-Mg-Cu alloy (7050)*. Acta Materialia, 2004. **52**(15): p. 4503-4516.

- [2] Liddicoat, P.V., et al., *Analysis of Vacancy Complexes in Al-Zn-Mg(-Cu) Alloys During Early Stages of Age Hardening*. Aluminium Alloys - Their Physical and Mechanical Properties, ed. J. Hirsch, B. Strotzki, and G. Gottstein. Vol. 1. 2008, Weinheim: Wiley-VCH Verlag GmbH & Co. KGaA.
- [3] Chinh, N.Q., et al., *The effect of Cu on mechanical and precipitation properties of Al-Zn-Mg alloys*. Journal of Alloys and Compounds, 2004. **378**(1-2): p. 52-60.
- [4] Liddicoat, P.V., S.K. Maloney, and S.P. Ringer, *Solute cluster and precipitate evolution during age-hardening of a 7000 Al alloy*. 2010: p. Under submission.
- [5] Polmear, I.J., J. Inst. Metals, 1957-58. **86**: p. 113.
- [6] Laves, F. and L. Lohberg, Nachr. Akad. Wiss. (Gottingen), 1934. **1**: p. 59.
- [7] Tarschisch, L., A.T. Titov, and F.K. Garjanov, Phys. Z. U.S.S.R., 1934. **5**: p. 503.
- [8] Mondolfo, L.F., N.A. Gjostein, and D.W. Lewinson, Trans. AIME, 1956. **206**: p. 1378.
- [9] Graf, R., Compt. Rend., 1957. **244**: p. 337.
- [10] Embury, J.D. and R.B. Nicholson, *The nucleation of precipitates: The system Al-Zn-Mg*. Acta Metallurgica, 1965. **13**(4): p. 403-417.
- [11] Thackery, P.A., J. Inst. Metals, 1968. **96**: p. 228.
- [12] Gjønnes, J. and C.J. Simensen, Acta Mat., 1970. **18**: p. 881.
- [13] Polmear, I.J., *The Ageing Characteristics of Complex Al-Zn-Mg Alloys*. J. Inst. Metals, 1960(89): p. 51.
- [14] Dix Jr., E.H., Trans. Amer. Soc. Met., 1950. **52**: p. 1057.
- [15] Caraher, S.K., I.J. Polmear, and S.P. Ringer, *Effects of Cu and Ag on precipitation in Al-4Zn-3Mg (wt. %)*. Proceedings of ICAA-6, 1998: p. 739-744.
- [16] Maloney, S.K., I.J. Polmear, and S.P. Ringer, *Effects of Cu on precipitation in Al-Zn-Mg alloys*. Materials Science Forum, 2000. **331** (II): p. 1055-1060.
- [17] Silcock, J.M., J. I. Met., 1960-61. **89**: p. 203.
- [18] Bagaryatshy, Y.A., Dokl Akad SSSR, 1952. **87**: p. 397.
- [19] Wolverson, C., *Crystal structure and stability of complex precipitate phases in Al-Cu-Mg-(Si) and Al-Zn-Mg alloys*. Acta Materialia, 2001. **49**(16): p. 3129-3142.
- [20] Ringer, S.P., T. Sakurai, and I.J. Polmear, *Origins of hardening in aged Al-Cu-Mg-(Ag) alloys*. Acta Materialia, 1997. **45**(9): p. 3731-3744.
- [21] Starink, M.J., et al., *Room temperature precipitation in quenched Al-Cu-Mg alloys: a model for the reaction kinetics and yield strength development*. Philosophical Magazine, 2005. **85**(13): p. 1395 - 1417.
- [22] Perlitz, H. and A. Westgren, Arkiv Kemi Mineral Geol, 1943. **16B**: p. 13.
- [23] Marceau, R.K.W., G. Sha, and S.P. Ringer, *Cluster Hardening in Al-Cu-Mg Alloys: Analysis of Cu-Mg Atomic Clustering, in Aluminium Alloys: Their Physical and Mechanical Properties*. 2008, Wiley-VCH Verlag GmbH & Co. KGaA: Weinheim.
- [24] Ringer, S.P., et al., *Cluster hardening in an aged Al-Cu-Mg alloy*. Scripta Materialia, 1997. **36**(5): p. 517-521.
- [25] Liddicoat, P.V., et al., *Evolution of Nanostructure During the Early Stages of Ageing in Al-Zn-Mg-Cu Alloys*. Mater. Sci. For., 2006. **519-521**: p. 555-560.
- [26] Polmear, I.J., *The upper temperature limit of stability of G.P. zones in ternary aluminium-zinc-magnesium alloys*. J. Inst. Metals, 1958. **87**: p. pp. 24-25.
- [27] Katz, Z. and N. Ryum, *Precipitation kinetics in Al-alloys*. Scripta Metall. Mater., 1981. **15**(3): p. 265-268.
- [28] Hart, E.W., *On the role of point defects in some low temperature reactions*. Acta Metallurgica, 1958. **6**(8): p. 553-553.
- [29] Ryum, N., *Precipitation Kinetics in an Al-Zn-Mg-Alloy*. Z. Metallkde., 1975. **66**: p. 338.
- [30] Stephenson, L.T., et al., *New Techniques for the Analysis of Fine-Scaled Clustering Phenomena within Atom Probe Tomography (APT) Data*. Microsc. Microanal., 2007. **13**: p. 448-463.
- [31] Gault, B., et al., *Estimation of the Reconstruction Parameters for Atom Probe Tomography*. Microsc. Microanal., 2008. **14**(4): p. 296-305.
- [32] Hirsch, P.B., et al., *Electron Microscopy of Thin Crystals*. 1977, New York: Krieger.
- [33] Miller, M.K., *Atom Probe Tomography: Analysis at the Atomic Level*. 2000, New York: Springer.
- [34] Moody, M.P., et al., *Contingency table techniques for three dimensional atom probe tomography*. Microscopy Research and Technique, 2007. **70**(3): p. 258-268.
- [35] Williams, D.B. and C.B. Carter, *Transmission electron microscopy*. 1996, New York and London: Plenum Press.
- [36] Nie, J., et al., *On the roles of clusters during intragranular nucleation in the absence of static defects*. Metallurgical and Materials Transactions A, 2002. **33**(6): p. 1649-1658.